

## UVIT/AstroSat observation of TW Hya

PRASANTA K. NAYAK,<sup>1,2</sup> MAYANK NARANG,<sup>3,2</sup> P. MANOJ,<sup>2</sup> D. K. OJHA,<sup>2</sup> BLESSON MATHEW,<sup>4</sup> T. BAUG,<sup>5</sup> S. CHANDRA,<sup>2</sup>  
S. VIG,<sup>6</sup> G. MAHESWAR,<sup>7</sup> AND U. S. KAMATH<sup>7</sup>

<sup>1</sup>*Instituto de Astrofísica, Pontificia Universidad Católica de Chile, Av. Vicuña MacKenna 4860, 7820436, Santiago, Chile*

<sup>2</sup>*Department of Astronomy and Astrophysics, Tata Institute of Fundamental Research, Mumbai, 400005, India*

<sup>3</sup>*Academia Sinica Institute of Astronomy & Astrophysics, 11F of Astro-Math Bldg., No.1, Sec. 4, Roosevelt Rd., Taipei 10617, Taiwan, R.O.C.*

<sup>4</sup>*Department of Physics and Electronics, CHRIST (Deemed to be University), Bangalore 560029, India*

<sup>5</sup>*S. N. Bose National Centre for Basic Sciences, Sector-III, Salt Lake, Kolkata 700106, India*

<sup>6</sup>*Indian Institute of Space science and Technology, Thiruvananthapuram 695547, India*

<sup>7</sup>*Indian Institute of Astrophysics, Bangalore, 560034, India*

### ABSTRACT

The paper demonstrates the spectroscopic and photometric capabilities of the Ultra-Violet Imaging Telescope (UVIT) to study T-Tauri stars (TTSs). We present the first UVIT/Far-UV spectrum of a TTS, TW Hya. Based on C IV line luminosity, we estimated accretion luminosity ( $0.1 L_{\odot}$ ) and mass accretion rate ( $2.2 \times 10^{-8} M_{\odot}/yr$ ) of TW Hya, and compared these values with the accretion luminosity ( $0.03 L_{\odot}$ ) and mass accretion rate ( $0.6 \times 10^{-8} M_{\odot}/yr$ ) derived from spectral energy distribution (SED). From the SED, we derive best-fitted parameters for TW Hya:  $T_{eff} = 3900 \pm 50$  K, radius =  $1.2 \pm 0.03 R_{\odot}$ ,  $\log g = 4.0$  and equivalent black-body temperatures corresponding to accretion luminosity as  $14100 \pm 25$  K. The parameters of TW Hya derived from UVIT observations were found to be matched well with the literature. Comparison with IUE spectra also suggests that UVIT can be used to study the spectroscopic variability of young stars. This study proposes leveraging the FUV spectroscopic capabilities of UVIT to contribute to the advancement of upcoming UV spectroscopic missions, including the Indian Spectroscopic Imaging Space Telescope.

*Keywords:* stars: pre-main sequence

### 1. INTRODUCTION

T-Tauri Stars (TTSs) show signs of enhanced line emission (e.g., emission from Ca IR triplet, Hydrogen Balmer lines) in the optical wavelength (Joy 1945). These lines can be used to trace the mass accretion and outflow rates from these TTSs (e.g., Muzerolle et al. 1998a; Stahler & Palla 2004; Hartmann et al. 2016; Alcalá et al. 2021). The TTSs also show a strong continuum excess long-ward of about  $1 \mu\text{m}$ , indicating the presence of the protoplanetary disk around them. Apart from showing strong line emission and IR excess, TTSs also emit significant excess in the blue and UV continuum (Kuhi 1974; Schneider et al. 2020). These blue and UV excesses in classical TTSs (CTTSs) are attributed to

accretion shocks (Walker 1972; Hartmann et al. 2016). These shocks are produced by the accretion column hitting the stellar surface and heating the infalling material to temperatures  $> 10^6$  K, resulting in the generation of a copious amount of X-ray radiation, which gets partly reprocessed into UV and optical continuum radiation (Hartmann et al. 2016). The strong emission lines are mainly produced in the extended magnetospheric infall region, while some lines are also produced in the accretion shock as well (Hartmann et al. 2016). A typical CTTS spectrum consists of line and continuum emissions from the accretion flow and shock, along with emissions from the chromospheric (stellar) activity and the stellar photosphere.

Traditionally, accretion rates onto CTTSs have been derived using the optical emission lines, the blue excess, and veiling in the optical regime (e.g., Muzerolle et al. 1998b; Rigliaco et al. 2012; Hartmann et al. 2016; Alcalá et al. 2021). However, X-ray and UV observa-

tions offer the most direct method for measuring the accretion process in low-mass stars. The emission from hot plasma originates due to the accretion shock and emits most of its energy in the UV range (Appenzeller & Wolf 1979). The UV spectra also have several disk features such as fluorescently excited  $\text{H}_2$  and CO emissions (e.g., Herczeg et al. 2002; Schindhelm et al. 2012) as well as atomic lines from the hot post-shock region of jets and from wide-angle outflows (e.g., Schneider et al. 2013). All these developments in the UV analysis of CTTS came with the advent of the International Ultraviolet Explorer (IUE) satellite (Bogges et al. 1978), which was later followed up by data from the Hubble Space Telescope (HST).

The NUV and FUV spectra of CTTSs are dominated by strong emission lines from ionized species such as  $\text{O I } \lambda 1304$ , the  $\text{Si IV } \lambda\lambda 1394/1403$  doublet, the  $\text{C IV } \lambda\lambda 1548/1450$  doublet,  $\text{He II } \lambda 1640$ ,  $\text{Mg II } \lambda 2800$  complex and  $\text{C II } \lambda\lambda 2323/2324$  doublet (Valenti et al. 2000; Johns-Krull et al. 2000; Valenti et al. 2003). Yang et al. (2012) found a strong correlation between the line luminosity of some of these hot ionic lines and the accretion traces such as the Balmer lines and the  $\text{Ca II K}$  line in the optical. They also found that the FUV continuum luminosity strongly correlates with the accretion luminosity (also see Ingleby et al. 2011). Similar results connecting the UV luminosity to accretion luminosity have also been derived using broadband photometry by Nayak et al. (2024). Recently, a large HST UV spectroscopic program was also initiated by the STScI Director in 2019 to study the accretion processes in young high- and low-mass stars in the local universe, named Ultraviolet Legacy Library of Young Stars as Essential Standards (ULLYSES), which was completed in 2023. Overall, this shows the strength of FUV luminosity as a tool to study the accretion onto pre-main-sequence stars.

In this work, we examine the spectroscopic capabilities of the Ultra-Violet Imaging Telescope (UVIT) to study TTSs and discuss if the UVIT can be used to complement the legacy of the ULLYSES program in future. Nayak et al. (2024) recently demonstrated the photometric capabilities of UVIT to study the accretion mechanism in TTSs. However, the spectroscopic capabilities of UVIT to study TTS have not been explored yet. In this paper, we use the UVIT data of TW Hya to explore this. We have organized the paper in the following way: in Section 2, we discuss the properties of TW Hya; observation and data reduction are mentioned in section 3; results are discussed in section 4 and summarized in section 5.

## 2. TW HYA

TW Hya is a CTTS and is the most prominent member of the TW Hya association (Kastner et al. 1997). Its spectral type ranges from K6/K7 to M2 ( $T_{\text{eff}} = 4200 - 3600$  K) depending on whether measured in blue/optical or near-IR wavelengths (Webb et al. 1999; Yang et al. 2005; Vacca & Sandell 2011; Debes et al. 2013; McClure et al. 2013; Venuti et al. 2019). TW Hya is also the closest T-Tauri star at 60.14 pc (Bailer-Jones et al. 2021). It is located in a region devoid of dark and CO clouds and is an isolated TTSs (Rucinski & Krautter 1983). Due to this, the extinction ( $A_V$ ) towards TW Hya is negligible. Even though the system is about 5-10 Myr old, there is still IR excess associated with it, indicating the presence of a protoplanetary disk, which has been imaged with HST (e.g., Debes et al. 2017), ground-based coronagraphs (e.g., Akiyama et al. 2015; Rapson et al. 2015) and ALMA (e.g., Andrews et al. 2016; Huang et al. 2018) in great detail. The disk structure of TW Hya includes a dust-depleted inner hole, as well as a series of bright rings, with the closest one located at about one astronomical unit (1 AU) from the star. This makes TW Hya a transitional disk candidate (Uchida et al. 2004; Andrews et al. 2016). These gaps are thought to be created due to the ongoing planet formation in the disk. The relatively old age of the system ( $\sim 5-10$  Myr) for a T-Tauri star makes it a candidate for long-lived disks. Understanding the accretion processes in such long-lived disk systems can provide important clues about the fate of planetary systems.

TW Hya has previously been observed in the UV wavelength with IUE and HST (Herczeg et al. 2002; Robinson & Espaillat 2019). The UV flux from TW Hya is also found to be variable (Robinson & Espaillat 2019), which indicates that the mass accretion from TW Hya might also be changing with time. Furthermore, several campaigns using ground-based telescopes have targeted the system to study the mass accretion processed onto the star (e.g., Venuti et al. 2019). In a recent study, Herczeg et al. (2023) combined high-resolution spectroscopic data (from UV to IR) obtained over 25 years to understand the variable accretion mechanism in TW Hya.

## 3. OBSERVATIONS AND DATA REDUCTION

UVIT has a low-resolution slit-less spectroscopic facility in both NUV and FUV bands: one grating is mounted in the NUV wheel and two gratings (with orthogonal dispersions axes) in the FUV wheel. However, the NUV channel is currently inoperative and only the FUV channel remains operative. The maximum efficiency is achieved in the  $-2$  order of the FUV gratings

**Table 1.** The AstroSat/UVIT observations log with the filter range and exposure time.

UVIT Filter	Wavelength range (Å)	Exposure (s)
NUVB13 (N245M)	2195.08 — 2634.78	5197
NUVN2 (N279N)	2722.26 — 2877.19	2951
NUV Silica-1 (N242W)	1700.00 — 3050.00	1845
FUV Grating 1	1200.00 — 1800.00	8062

with a spectral resolution of 15 Å (Tandon et al. 2020; Dewangan 2021).

The UVIT observations of TW Hya were carried out as part of the GT proposal (ID: G07\_086, PI: D. K. Ojha) on 2017 April 07. The FUV observation was performed in the spectroscopic mode, while the NUV observations were completed in the photometric mode in a wide (N242W/Silica-1), a medium (N245M/NUVB13), and a narrow (N279N/NUVN2) band. The details of these filters and the corresponding exposure times in those filters are shown in Table 1.

Both the photometric and spectroscopic observations were completed in multiple orbits. The level1 raw data was corrected for spacecraft drift, flat-field and distortion, and the orbit-wise images were generated using the software CCDLAB (Postma & Leahy 2017). Then, the orbit-wise images were co-aligned and combined to generate final science-ready images in each filter. Astrometry was also performed using CCDLAB by comparing the *Gaia*-DR2 source catalogue. The details about the telescope and the instruments are available in Subramaniam et al. (2016); Tandon et al. (2017a) and the instrument calibration can be found in Tandon et al. (2017b, 2020).

For the photometric data reduction, we used the DAOPHOT tasks and packages in the Image Reduction and Analysis Facility (IRAF) software (Stetson 1987). As the observed field is not crowded, we performed aperture photometry and applied aperture corrections to aperture magnitudes. The final magnitudes are calculated in the AB magnitude system by adding zero-point magnitudes for the corresponding bands, obtained from Tandon et al. (2020). In the case of slit-less spectroscopic observation, we used m=-2 order, as shown in Figure 1, for further analysis. The wavelength and flux calibrated spectrum is generated using the pipeline by

Dewangan (2021). The spectrum is shown in the top panel of Figure 2.

## 4. RESULTS

### 4.1. FUV spectrum of TW Hya

In the top panel of Figure 2, we have shown the FUV/UVIT spectrum of TW Hya. The spectrum clearly shows the detection of several strong lines such as O I  $\lambda$ 1304, the Si IV  $\lambda$  $\lambda$ 1394/1408 doublet, the C IV  $\lambda$ 1549 doublet, and the He II  $\lambda$ 1640. We have also compared the spectrum with low-resolution IUE spectra and high-resolution HST spectra obtained from the archive in the middle and bottom panel of Figure 2, respectively. Before comparing with the HST spectra, we degraded its spectral resolution to UVIT resolution. The epochs of these observations are also mentioned in the figure. The FUV/UVIT spectrum matches well with both IUE and HST spectra in terms of line detection, however, due to relatively lower resolution ( $\sim$ 15 Å; Dewangan 2021) than IUE, the FUV/UVIT spectrum is unable to resolve the O III emission. The multi-epoch spectra from both IUE and HST show the signature of variation in the continuum as well as line flux. The UVIT spectrum is found to match nicely with one of the epochs for both IUE and HST. Part of this variability could be attributed to the variable accretion rate. However, some of the variability could be due to uncertainty in the flux calibration. Multiple IUE observations of the same target showed that the flux at different epochs is within 10 % (Bohlin & Bianchi 2018). This is much larger than the offset seen between the two IUE epochs of TW Hya. For UVIT, the flux uncertainty is higher ( $\sim$ 21-25%). This uncertainty is still (factor of  $\sim$  2) smaller than the variation in IUE flux observed in the two epoch. This shows a clear signature of accretion variability of TW Hya and indicates that UVIT FUV spectra can be used to detect the variable accretion despite of relatively large uncertainty in continuum flux. In Table 2, we list the line fluxes from the TW Hya system for the three epochs. We measured line fluxes by subtracting the continuum estimated with a linear fit with wavelength and subsequently integrating the emission remaining in the line. The uncertainty in the line flux is computed based on the uncertainty in the flux.

### 4.2. Mass accretion rates from FUV spectroscopy

The C IV line present in the FUV spectrum is an accretion tracer and can be used to compute the mass accretion rate onto T-Tauri stars. The C IV line also correlates with the accretion luminosity as well as FUV luminosity. Following Yang et al. (2012) we can express

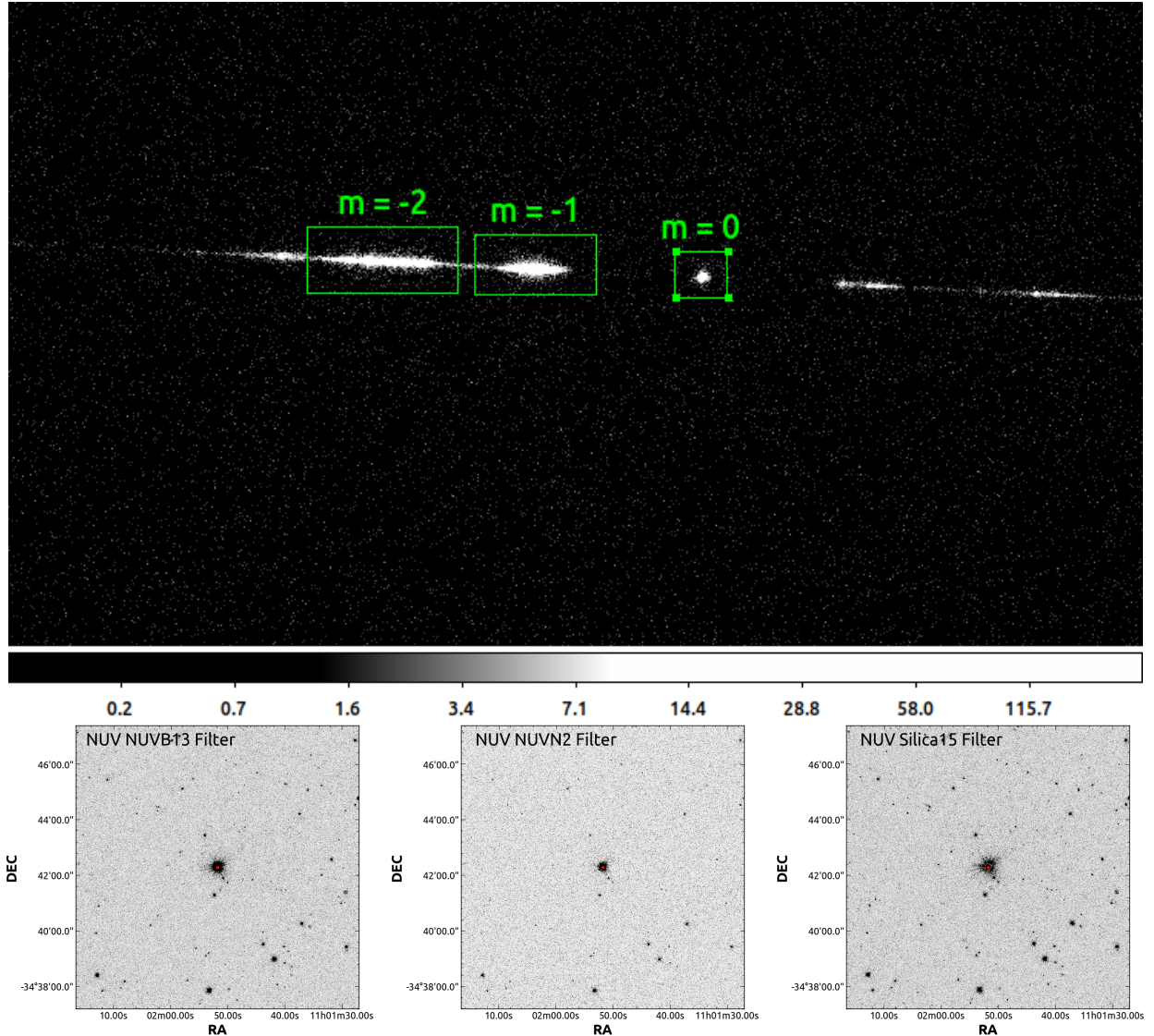


**Figure 1.** (top panel) FUV Grating-1 image of TW Hya. (bottom panel) NUV images of TW Hya in different UVIT filters.

the line luminosity of the C IV  $\lambda$  1549 line as a function of accretion luminosity:

$$\log(L_{C\text{ IV}}) = -2.766 + 0.877 \times \log(L_{\text{acc}}) \quad (1)$$

Using the line fluxes listed in Table 2, we compute the  $L_{\text{acc}}$  from the UVIT and IUE spectra. We derive an  $L_{\text{acc}}$  of  $0.1 L_{\odot}$  from the UVIT spectrum while from the IUE spectra we derive an  $L_{\text{acc}}$  between  $0.04 - 0.06 L_{\odot}$  and from the degraded HST spectra  $L_{\text{acc}}$  lie between  $0.04 - 0.1 L_{\odot}$ . We notice that the value of  $L_{\text{acc}}$  from UVIT observation matches well with that obtained from IUE and HST.

The accretion luminosity  $L_{\text{acc}}$  can then be converted into the mass accretion rate following Gullbring et al. (1998) :

$$L_{\text{acc}} = \frac{G M_* \dot{M}_{\text{acc}}}{R_*} \left( 1 - \frac{R_*}{R_{in}} \right) \quad (2)$$

where  $M_*$  and  $R_*$  are the mass and radius of the star,  $\dot{M}_{\text{acc}}$  is the mass accretion rate and  $R_{in}$  is the dust truncation radius. The typical value for  $R_{in}$  is  $R_{in} = 5R_*$  and for  $R_*/M_* \sim 5R_{\odot}/M_{\odot}$  (Muzerolle et al. 1998a). Using Equation 2, we derive the mass accretion rate onto TW Hya to be between  $8.6 - 21.7 \times 10^{-9} M_{\odot}/\text{yr}$ . Similar values for mass accretion rates have been derived for TW Hya using various other techniques (e.g., Kastner et al. 1997; Venuti et al. 2019; Robinson & Espaillat 2019).

### 4.3. SED analysis

The accretion process in TTSs causes excess radiation in the UV region and the accretion luminosity peaks in

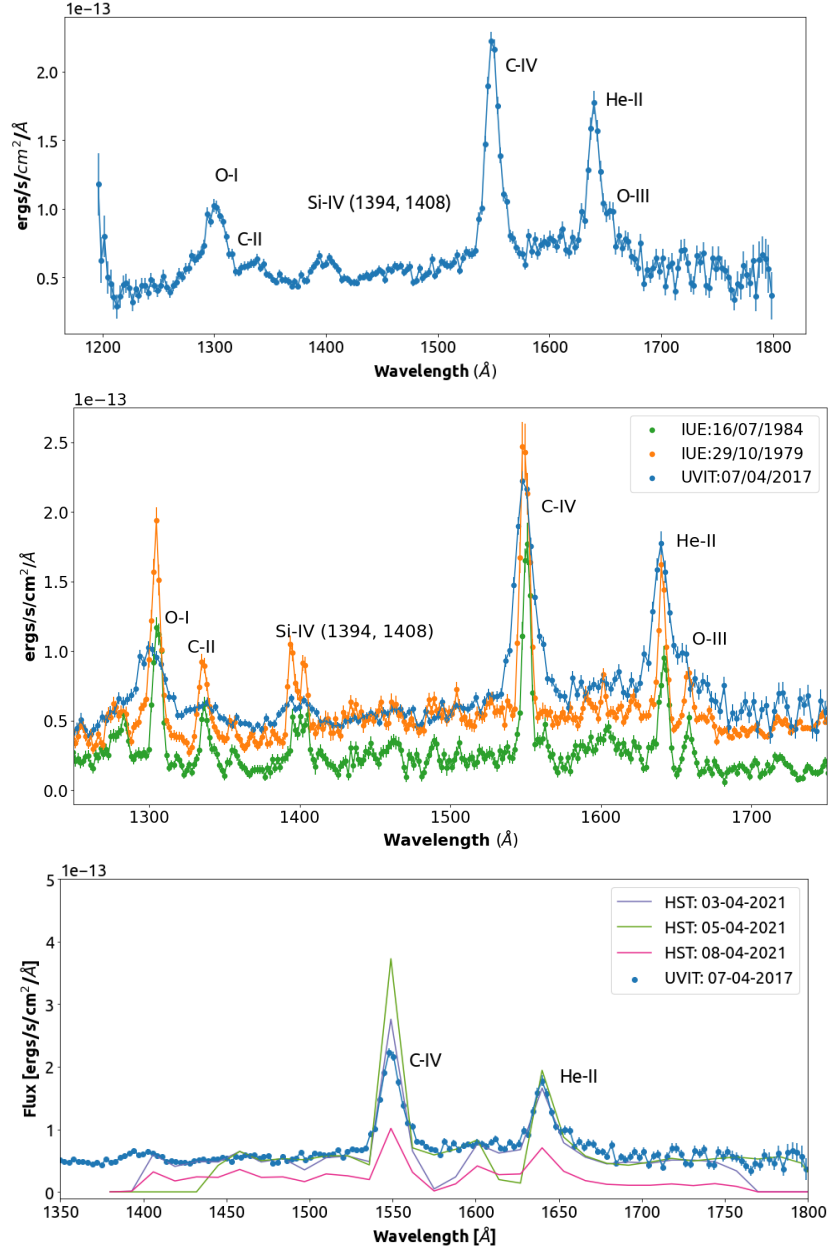


**Figure 2.** (Top panel): UVIT/FUV spectrum of TW Hya. (Middle panel): UVIT spectrum is compared with the low-resolution IUE spectra of two epochs. (Bottom panel): UVIT spectrum is compared with the HST spectra (from the ULLYSES archive) of three epochs, where HST spectra are degraded to UVIT resolution.

the FUV region with equivalent black body temperature  $\sim 10^4$  K (Calvet & Gullbring 1998). Simultaneous FUV and NUV observation will provide a better estimation of UV luminosity (due to accretion or chromospheric activity) by constructing spectral energy distribution (SED) and measuring excess emission over photospheric luminosity. Simultaneous FUV and NUV observations also help us to estimate the equivalent temperature corresponding to UV luminosity by comparing the excess UV luminosity with a black body SED (Nayak et al.

2024). As TW Hya is observed simultaneously in FUV and NUV filters, we tried to estimate the accretion luminosity and its corresponding peak temperature by performing a two-component model spectra that fit the UV and optical part of the SED of TW Hya.

The TW Hya is detected in all three NUV/UVIT filters, however, it gets saturated in the NUV Silica-1 and NUVB13 filters. Therefore, we used NUV photometry only in the NUVN2 band. To get the FUV magnitudes in different UVIT filters, we convolved the FUV

**Table 2.** The line flux measured from the UVIT and archival IUE spectra.

Line	Wavelength	Line Flux ( $\times 10^{-13}$ ergs/s/cm <sup>2</sup> )		
		UVIT	IUE	
		2017 April 07	1979 October 29	1984 July 16
O I	1302.168	$6.5 \pm 0.8$	$11.7 \pm 1.4$	$6.7 \pm 1.2$
C II doublet	1334.532 - 1335.708	—	$4.7 \pm 1$	$3.4 \pm 0.9$
Si IV doublet	1393.755 - 1402.770	—	$6.7 \pm 1.1$	$4.1 \pm 0.9$
C IV doublet	1548.187 - 1550.772	$21.8 \pm 1.3$	$14.4 \pm 1.7$	$9.7 \pm 1.3$
He II	1640.420	$12.1 \pm 1.1$	$6.3 \pm 0.8$	$5.6 \pm 0.9$
O [III]	1660.809	$2.6 \pm 0.5$	$2.2 \pm 0.5$	$1.8 \pm 0.5$

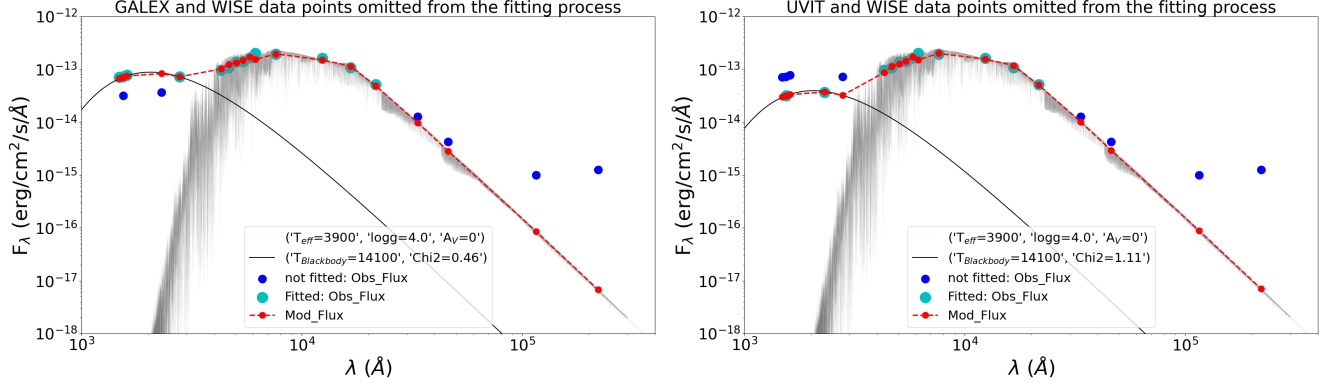


**Figure 3.** SEDs of TW Hya are shown here. The grey and black lines represent the best-fitted synthetic black body and dwarf spectra, respectively, on observed fluxes (cyan and blue points). Cyan points are included in the fitting algorithm, but omitting the blue points. The red dashed line indicates the expected combined model flux from the fitted synthetic spectra. (left), we omitted GALEX and WISE data in the fitting process. (right), we omitted UVIT and WISE data. The best-fitted parameters are mentioned in the legends.

spectrum with the corresponding filter response curve and obtained FUV magnitudes in F148W, F154W, and F169M bands. To construct the SED, we have included available photometric data from the archive along with AstroSat/UVIT data points, which are GALEX GR6+7 (Bianchi et al. 2017), *Gaia*-DR3 (Gaia Collaboration et al. 2021; Babusiaux et al. 2022), APASS DR9 (Henden et al. 2015), 2MASS (Skrutskie et al. 2006), and WISE (Wright et al. 2010). We have used virtual observatory (VO) tool, VOSA (VO SED Analyzer; Bayo et al. (2008)) developed by Spanish Virtual Observatory to generate SEDs and to fit theoretical model spectra of a black body and a dwarf star (BT-Settl-CIFIST model; Allard et al. 2011) in the UV and optical regions of the observed flux distribution. We did not include WISE data points in IR regions for the SED fit as a substantial excess emission in the near-IR region comes from the disk. We have used  $\log g$  values between 4 to 5 and full  $T_{eff}$  range of 1200 to 7000 K with a resolution of 100 K for the BT-Settl-CIFIST model. In the case of black body, we used spectra for a range of 5000 to 20000 K with a resolution of 50 K. We kept  $A_v$  as a free parameter in the fitting process.

From the literature, we know that TW Hya has a variable accretion rate (Robinson & Espaillat 2019). As the signature of accretion variability is more prominent in UV compared to optical and also UV observations from GALEX and UVIT belonging to two different epochs, we perform the SED fit twice. First, we include only UVIT data points in the UV region for the fitting, and secondly, we include only the GALEX data points in the UV region. The SED and the best fit to the SED for TW Hya are shown in Figure 3. We notice that VOSA provides very similar stellar parameters for both the fittings but with a large deviation in UV or black-body luminosity. From both the SEDs, we derive the best fit  $T_{eff}$  of  $3900 \pm 50$  K for TW Hya and  $\log g = 4.0$ . This is similar to the  $T_{eff}$  reported in the literature for the star (Venuti et al. 2019). We found  $A_v = 0$  which supports the results of Herczeg et al. (2004) and also with the Gaia catalog (Gaia Collaboration et al. 2021).

We found the black-body temperature from both the SEDs to be the same as  $14100 \pm 25$  K but UV luminosity (i.e. accretion luminosity,  $L_{acc}$ ) is more than twice in the case of UVIT data ( $0.031 \pm 0.002 L_{\odot}$ ) compared to that for GALEX data ( $0.014 \pm 0.002 L_{\odot}$ ). The values match well with that estimated using C IV line luminosity and

also with the literature (see Table 7 in [Herczeg et al. 2023](#)). As TW Hya is still accreting, UV excess generated due to the accretion shocks is expected from the system. However, we notice a small deviation in optical luminosity (i.e. the luminosity of TW Hya) between two different fitting:  $0.30 L_{\odot}$  for the SED with UVIT data and  $0.31 L_{\odot}$  for the SED with GALEX. While the source shows similar optical luminosity over two epochs, the accretion luminosity has a significant variation. This finding not only confirms the presence of accretion variability in TW Hya but also demonstrates the importance of SED analyses to probe the accretion variability in TTS. The observed flux measurements are denoted as cyan and blue points, where cyan points fall in the UV and optical region of the energy distribution which are included in the dual component fitting of model spectra. The blue points are not included in the fitting process. The black and grey lines represent the best-fitted black-body and BT-Settl-CIFIST spectra, respectively to the cyan points. The combined fluxes from these two model spectra in different wavebands are denoted in red and connected with the red dotted line. The overlap between red and cyan points indicates the goodness of the dual fitting. The values of reduced  $\chi^2$ , temperatures,  $\log g$  corresponding to the best-fitted spectra are also noted in the legends.

We further estimated the mass accretion rate from accretion luminosity using the [Equation 2](#). We find the accretion rate of TW Hya as  $6.2 \times 10^{-9} M_{\odot}/yr$  (for the SED fit with UVIT data) and  $2.8 \times 10^{-9} M_{\odot}/yr$  (for the SED fit with GALEX data). The values match well with our spectroscopic analysis, as well as with the literature values ([Venuti et al. 2019](#); [Robinson & Espaillat 2019](#); [Herczeg et al. 2023](#)). We also compute the filling factor (area of the UV emitting region/ area of the star) to be 0.18% (for the SED fit with UVIT data) and 0.08% ((for the SED fit with GALEX data)). This is comparable to the filling factor derived for TW Hya of 0.26% by [Ingleby et al. \(2013\)](#) and to the filling factor of other T-Tauri stars.

## 5. SUMMARY

We present the first UVIT/FUV spectrum of a T Tauri star, TW Hya. TW Hya is observed in NUV with UVIT but in the photometric mode. The UVIT/FUV spectrum matches well with the low-resolution IUE spectrum. Combining the IUE observations with the UVIT, we found that the line flux, as well as the continuum, is variable in FUV. This indicates the variable nature of the mass accretion rate in TW Hya. Using the C IV line luminosities from IUE and UVIT spectroscopic observations, we measured the range in accretion luminosity

( $0.04 - 0.1 L_{\odot}$ ) and mass accretion rates ( $8.6 - 21.7 \times 10^{-9} M_{\odot}/yr$ ) onto TW Hya.

We performed SED analysis of TW Hya using photometric observations to estimate stellar parameters (luminosity, temperature, radius,  $\log g$ ), UV/accretion luminosity and its corresponding temperature. We also performed another SED analysis using GALEX observation, not including UVIT. We found that the accretion luminosity value using UVIT observation ( $0.031 L_{\odot}$ ) is more than two times compared to that found using GALEX observation ( $0.014 L_{\odot}$ ). This also supports the variable accretion nature of TW Hya. However, other parameters found to be similar using both the observations:  $T_{eff} = 3900$  K;  $\log g = 4.0$ , radius =  $1.2 R_{\odot}$ , black-body temperature corresponding to accretion luminosity =  $14100$  K. From SED analysis using photometric observations, we found the mass accretion rate ranges between  $2.8 - 6.2 \times 10^{-9} M_{\odot}/yr$ .

This study demonstrates both spectroscopic and photometric capabilities of UVIT to study young stars. Though there are many studies on young stars/star-forming regions using UVIT photometry, the spectroscopy capabilities of UVIT have not been explored to their full potential, especially in the case of young stars. Comparison with IUE spectra also suggests that UVIT can be used to study the spectroscopic variability of young stars. UVIT spectroscopy, in conjunction with the HST observations, can provide an unprecedented view of the high-energy processes associated with star formation and provide complementary observations to the ULLYSES program. This work also highlights the need of developing future UV spectroscopic missions such as the Indian Spectroscopic Imaging Space Telescope (INSIST; [Subramaniam 2022](#)) to study the accretion process associated with star formation.

This publication uses UVIT data from the AstroSat mission of the ISRO, archived at the Indian Space Science Data Centre (ISSDC). The UVIT project is a result of collaboration between IIA, Bengaluru, IUCAA, Pune, TIFR, Mumbai, several centres of ISRO, and CSA. This publication uses UVIT data processed by the payload operations centre by the IIA. PKN acknowledges TIFR's postdoctoral fellowship. PKN also acknowledges support from the Centro de Astrofísica y Tecnologías Afines (CATA) fellowship via grant Agencia Nacional de Investigación y Desarrollo (ANID), BASAL FB210003. DKO acknowledges the support of the Department of Atomic Energy, Government of India, under Project Identification No. RTI 4002.

*Software:* astropy (Astropy Collaboration et al. 2013, 2018), CCDLAB (Postma & Leahy 2017)

## REFERENCES

- Akiyama, E., Muto, T., Kusakabe, N., et al. 2015, *ApJL*, 802, L17, doi: [10.1088/2041-8205/802/2/L17](https://doi.org/10.1088/2041-8205/802/2/L17)
- Alcalá, J. M., Gangi, M., Biazzo, K., et al. 2021, *A&A*, 652, A72, doi: [10.1051/0004-6361/202140918](https://doi.org/10.1051/0004-6361/202140918)
- Allard, F., Homeier, D., & Freytag, B. 2011, in *Astronomical Society of the Pacific Conference Series*, Vol. 448, 16th Cambridge Workshop on Cool Stars, Stellar Systems, and the Sun, ed. C. Johns-Krull, M. K. Browning, & A. A. West, 91. <https://arxiv.org/abs/1011.5405>
- Andrews, S. M., Wilner, D. J., Zhu, Z., et al. 2016, *ApJL*, 820, L40, doi: [10.3847/2041-8205/820/2/L40](https://doi.org/10.3847/2041-8205/820/2/L40)
- Appenzeller, I., & Wolf, B. 1979, *A&A*, 75, 164
- Astropy Collaboration, Robitaille, T. P., Tollerud, E. J., et al. 2013, *A&A*, 558, A33, doi: [10.1051/0004-6361/201322068](https://doi.org/10.1051/0004-6361/201322068)
- Astropy Collaboration, Price-Whelan, A. M., Sipőcz, B. M., et al. 2018, *AJ*, 156, 123, doi: [10.3847/1538-3881/aabc4f](https://doi.org/10.3847/1538-3881/aabc4f)
- Babusiaux, C., Fabricius, C., Khanna, S., et al. 2022, arXiv e-prints, arXiv:2206.05989. <https://arxiv.org/abs/2206.05989>
- Bailer-Jones, C. A. L., Rybizki, J., Fouesneau, M., Demleitner, M., & Andrae, R. 2021, *AJ*, 161, 147, doi: [10.3847/1538-3881/abd806](https://doi.org/10.3847/1538-3881/abd806)
- Bayo, A., Rodrigo, C., Barrado Y Navascués, D., et al. 2008, *A&A*, 492, 277, doi: [10.1051/0004-6361:200810395](https://doi.org/10.1051/0004-6361:200810395)
- Bianchi, L., Shiao, B., & Thilker, D. 2017, *ApJS*, 230, 24, doi: [10.3847/1538-4365/aa7053](https://doi.org/10.3847/1538-4365/aa7053)
- Boggess, A., Carr, F. A., Evans, D. C., et al. 1978, *Nature*, 275, 372, doi: [10.1038/275372a0](https://doi.org/10.1038/275372a0)
- Bohlin, R. C., & Bianchi, L. 2018, *AJ*, 155, 162, doi: [10.3847/1538-3881/aaaecl](https://doi.org/10.3847/1538-3881/aaaecl)
- Calvet, N., & Gullbring, E. 1998, *ApJ*, 509, 802, doi: [10.1086/306527](https://doi.org/10.1086/306527)
- Debes, J. H., Jang-Condell, H., Weinberger, A. J., Roberge, A., & Schneider, G. 2013, *ApJ*, 771, 45, doi: [10.1088/0004-637X/771/1/45](https://doi.org/10.1088/0004-637X/771/1/45)
- Debes, J. H., Poteet, C. A., Jang-Condell, H., et al. 2017, *ApJ*, 835, 205, doi: [10.3847/1538-4357/835/2/205](https://doi.org/10.3847/1538-4357/835/2/205)
- Dewangan, G. C. 2021, *Journal of Astrophysics and Astronomy*, 42, 49, doi: [10.1007/s12036-021-09691-w](https://doi.org/10.1007/s12036-021-09691-w)
- Gaia Collaboration, Brown, A. G. A., Vallenari, A., et al. 2021, *A&A*, 649, A1, doi: [10.1051/0004-6361/202039657](https://doi.org/10.1051/0004-6361/202039657)
- Gullbring, E., Hartmann, L., Briceño, C., & Calvet, N. 1998, *ApJ*, 492, 323, doi: [10.1086/305032](https://doi.org/10.1086/305032)
- Hartmann, L., Herczeg, G., & Calvet, N. 2016, *ARA&A*, 54, 135, doi: [10.1146/annurev-astro-081915-023347](https://doi.org/10.1146/annurev-astro-081915-023347)
- Henden, A. A., Levine, S., Terrell, D., & Welch, D. L. 2015, in *American Astronomical Society Meeting Abstracts*, Vol. 225, American Astronomical Society Meeting Abstracts #225, 336.16
- Herczeg, G. J., Linsky, J. L., Valenti, J. A., Johns-Krull, C. M., & Wood, B. E. 2002, *ApJ*, 572, 310, doi: [10.1086/339731](https://doi.org/10.1086/339731)
- Herczeg, G. J., Wood, B. E., Linsky, J. L., Valenti, J. A., & Johns-Krull, C. M. 2004, *ApJ*, 607, 369, doi: [10.1086/383340](https://doi.org/10.1086/383340)
- Herczeg, G. J., Chen, Y., Donati, J.-F., et al. 2023, *ApJ*, 956, 102, doi: [10.3847/1538-4357/acf468](https://doi.org/10.3847/1538-4357/acf468)
- Huang, J., Andrews, S. M., Cleeves, L. I., et al. 2018, *ApJ*, 852, 122, doi: [10.3847/1538-4357/aaa1e7](https://doi.org/10.3847/1538-4357/aaa1e7)
- Ingleby, L., Calvet, N., Hernández, J., et al. 2011, *AJ*, 141, 127, doi: [10.1088/0004-6256/141/4/127](https://doi.org/10.1088/0004-6256/141/4/127)
- Ingleby, L., Calvet, N., Herczeg, G., et al. 2013, *ApJ*, 767, 112, doi: [10.1088/0004-637X/767/2/112](https://doi.org/10.1088/0004-637X/767/2/112)
- Johns-Krull, C. M., Valenti, J. A., & Linsky, J. L. 2000, *ApJ*, 539, 815, doi: [10.1086/309259](https://doi.org/10.1086/309259)
- Joy, A. H. 1945, *ApJ*, 102, 168, doi: [10.1086/144749](https://doi.org/10.1086/144749)
- Kastner, J. H., Zuckerman, B., Weintraub, D. A., & Forveille, T. 1997, *Science*, 277, 67, doi: [10.1126/science.277.5322.67](https://doi.org/10.1126/science.277.5322.67)
- Kuhi, L. V. 1974, *A&AS*, 15, 47
- McClure, M. K., Calvet, N., Espaillat, C., et al. 2013, *ApJ*, 769, 73, doi: [10.1088/0004-637X/769/1/73](https://doi.org/10.1088/0004-637X/769/1/73)
- Muzerolle, J., Hartmann, L., & Calvet, N. 1998a, *AJ*, 116, 2965
- . 1998b, *AJ*, 116, 455, doi: [10.1086/300428](https://doi.org/10.1086/300428)
- Nayak, P. K., Narang, M., Manoj, P., et al. 2024, arXiv e-prints, arXiv:2403.01935. <https://arxiv.org/abs/2403.01935>
- Postma, J. E., & Leahy, D. 2017, *PASP*, 129, 115002, doi: [10.1088/1538-3873/aa8800](https://doi.org/10.1088/1538-3873/aa8800)
- Rapson, V. A., Kastner, J. H., Millar-Blanchaer, M. A., & Dong, R. 2015, *ApJL*, 815, L26, doi: [10.1088/2041-8205/815/2/L26](https://doi.org/10.1088/2041-8205/815/2/L26)
- Rigliaco, E., Natta, A., Testi, L., et al. 2012, *A&A*, 548, A56, doi: [10.1051/0004-6361/201219832](https://doi.org/10.1051/0004-6361/201219832)
- Robinson, C. E., & Espaillat, C. C. 2019, *ApJ*, 874, 129, doi: [10.3847/1538-4357/ab0d8d](https://doi.org/10.3847/1538-4357/ab0d8d)
- Rucinski, S. M., & Krautter, J. 1983, *A&A*, 121, 217



- Schindhelm, R., France, K., Herczeg, G. J., et al. 2012, *ApJL*, 756, L23, doi: [10.1088/2041-8205/756/1/L23](https://doi.org/10.1088/2041-8205/756/1/L23)
- Schneider, P. C., Eisloffel, J., Güdel, M., et al. 2013, *A&A*, 550, L1, doi: [10.1051/0004-6361/201118592](https://doi.org/10.1051/0004-6361/201118592)
- Schneider, P. C., Günther, H. M., & France, K. 2020, *Galaxies*, 8, 27, doi: [10.3390/galaxies8010027](https://doi.org/10.3390/galaxies8010027)
- Skrutskie, M. F., Cutri, R. M., Stiening, R., et al. 2006, *AJ*, 131, 1163, doi: [10.1086/498708](https://doi.org/10.1086/498708)
- Stahler, S. W., & Palla, F. 2004, *The Formation of Stars*
- Stetson, P. B. 1987, *PASP*, 99, 191, doi: [10.1086/131977](https://doi.org/10.1086/131977)
- Subramaniam, A. 2022, *Journal of Astrophysics and Astronomy*, 43, 80, doi: [10.1007/s12036-022-09870-3](https://doi.org/10.1007/s12036-022-09870-3)
- Subramaniam, A., Tandon, S. N., Hutchings, J., et al. 2016, in *Proc. SPIE*, Vol. 9905, *Space Telescopes and Instrumentation 2016: Ultraviolet to Gamma Ray*, 99051F, doi: [10.1117/12.2235271](https://doi.org/10.1117/12.2235271)
- Tandon, S. N., Hutchings, J. B., Ghosh, S. K., et al. 2017a, *Journal of Astrophysics and Astronomy*, 38, 28, doi: [10.1007/s12036-017-9445-x](https://doi.org/10.1007/s12036-017-9445-x)
- Tandon, S. N., Subramaniam, A., Girish, V., et al. 2017b, *AJ*, 154, 128, doi: [10.3847/1538-3881/aa8451](https://doi.org/10.3847/1538-3881/aa8451)
- Tandon, S. N., Postma, J., Joseph, P., et al. 2020, *AJ*, 159, 158, doi: [10.3847/1538-3881/ab72a3](https://doi.org/10.3847/1538-3881/ab72a3)
- Uchida, K. I., Calvet, N., Hartmann, L., et al. 2004, *ApJS*, 154, 439, doi: [10.1086/422888](https://doi.org/10.1086/422888)
- Vacca, W. D., & Sandell, G. 2011, *ApJ*, 732, 8, doi: [10.1088/0004-637X/732/1/8](https://doi.org/10.1088/0004-637X/732/1/8)
- Valenti, J. A., Fallon, A. A., & Johns-Krull, C. M. 2003, *ApJS*, 147, 305, doi: [10.1086/375445](https://doi.org/10.1086/375445)
- Valenti, J. A., Johns-Krull, C. M., & Linsky, J. L. 2000, *ApJS*, 129, 399, doi: [10.1086/313408](https://doi.org/10.1086/313408)
- Venuti, L., Stelzer, B., Alcalá, J. M., et al. 2019, *A&A*, 632, A46, doi: [10.1051/0004-6361/201935745](https://doi.org/10.1051/0004-6361/201935745)
- Walker, M. F. 1972, *ApJ*, 175, 89, doi: [10.1086/151540](https://doi.org/10.1086/151540)
- Webb, R. A., Zuckerman, B., Platais, I., et al. 1999, *ApJL*, 512, L63, doi: [10.1086/311856](https://doi.org/10.1086/311856)
- Wright, E. L., Eisenhardt, P. R. M., Mainzer, A. K., et al. 2010, *AJ*, 140, 1868, doi: [10.1088/0004-6256/140/6/1868](https://doi.org/10.1088/0004-6256/140/6/1868)
- Yang, H., Johns-Krull, C. M., & Valenti, J. A. 2005, *ApJ*, 635, 466, doi: [10.1086/497070](https://doi.org/10.1086/497070)
- Yang, H., Herczeg, G. J., Linsky, J. L., et al. 2012, *ApJ*, 744, 121, doi: [10.1088/0004-637X/744/2/121](https://doi.org/10.1088/0004-637X/744/2/121)